Supplemental Table I: *Reported membrane potential values for various plant species and tissues under an array of physiologically relevant conditions published in the literature*

Plant species	***Tissue***	***Conditions***	***Reported MP range***	***Reference***
Arabidopsis thaliana (WT)	Root epidermis	Control	-114 – 125 mV	Bose et al (2015) Ann Bot
Arabidopsis thaliana (WT)	Root epidermis	Control 50 mM NaCl	-124 -128 mV -62 – 68 mV	Shabala et al (2005) Planta
Arabidopsis thaliana (GABA mutants)	Root epidermis	Control 100 mM NaCl	-92 -105 mV - 32 - 58 mV	Su et al (2019) J Exp Bot
Arabidopsis thaliana (HY mutants)	Root epidermis	Control 100 mM NaCl	-128-135 mV -25 – 52 mV	Bose et al (2013) J Exp Bot
Arabidopsis thaliana (WT)	Root epidermis	Control	-100 – 106 mV	Wu et al (2021) Plant Comm
Arabidopsis thaliana (WT)	Root epidermis	80 mM NaCl	- 48 – 93 mV	Cuin and Shabala (2007) Planta
Barley (various genotypes)	Root epidermis	Control 80 mM NaCl	-108 -110 mV -55 – 60 mV	Shabala et al (2016) Plant Physiol
Barley (>100 HD lines)	Root epidermis	Hypoxia	-40 -115 mV	Gill at el (2018) Frontiers Plant Sci
Barley (various genotypes)	Root epidermis	Control 80 mM NaCl	-118-122 mV -60 -78 mV	Bose et al (2014) Plant Cell Environ
Barley (various genotypes)	Root epidermis	Control 80 mM NaCl	- 122 – 129 mV - 46 – 82 mV	Chen et al (2007) Functional plant phys
Barley	Root stele	Control 20 mV NaCl	-116 – 118 mV - 70 – 80 mV	Shabala et al (2010) Plant J
Maize	Root epidermis	Control 100 mM NaCl	-114 – 118 mV -52 – 60 mV	Shabala et al (2009) Plant Cell Environ
Maize	Root stele	Control 100 mM NaCl	-121 – 138 mV -36 – 42 mV	Wegner et al (2011) Plant Cell Environ
Wheat	Root epidermis	control 80 mM NaCl	-120 -124 mV -60 - 64	Cuin et al (2008) J Exp Bot
Wheat	Root epidermis	Control 50 μM Al3+	-110 – 114 mV -102 -118 mV	Wherrett et al (2005) Funct Plant Biol
Atriplex	Root apex	Control 100 mM NaCl	-130 -132 mV 30 - 36 mV	Bose et al (2015) Ann Bot
Quinoa	Root apex	Control 100 mM NaCl	- 128 -130 mV -38 to - 42 mV	Bose et al (2015) Ann Bot
Thinoporium ponticum	Root epidermis	Control Anoxia	-105 – 100 mM -88 – 92 mV	Teakle et al (2013) Env Exp Bot
Bean	Mesophyll	Control	-106 -123 mV	Shabala et al (2000) J Exp Bot
Bean	Mesophyll	Control	-110 – 118 mV	Shabala et al (1999) Plant Physiol
Bean	Mesophyll	50 mM NaCl	- 38 - 42 mV	Percey et al (2014) Planta
Carpobrothus rossii	Mesophyll Storage parenchyma	Control Control	-62 -64 mV -68 -72 mV	Zeng et al (2018) Plant Cell Environ

Table I bibliography:

1. Shabala S, Newman I. Light-Induced Changes in Hydrogen, Calcium, Potassium, and Chloride Ion Fluxes and Concentrations from the Mesophyll and Epidermal Tissues of Bean Leaves. Understanding the Ionic Basis of Light-Induced Bioelectrogenesis. Plant Physiol. 1 mars 1999;119(3):1115‑24.

2. Shabala S, Babourina O, Newman I. Ion‑specific mechanisms of osmoregulation in bean mesophyll cells. Journal of Experimental Botany. juill 2000;51(348):1243‑53.

3. Shabala L, Cuin TA, Newman IA, Shabala S. Salinity-induced ion flux patterns from the excised roots of Arabidopsis sos mutants. Planta. déc 2005;222(6):1041‑50.

4. Wherrett T, Ryan PR, Delhaize E, Shabala S. Effect of aluminium on membrane potential and ion fluxes at the apices of wheat roots. Functional Plant Biol. 2005;32(3):199.

5. Chen Z, Zhou M, Newman IA, Mendham NJ, Zhang G, Shabala S. Potassium and sodium relations in salinised barley tissues as a basis of differential salt tolerance. Functional Plant Biol. 2007;34(2):150.

6. Cuin TA, Shabala S. Amino acids regulate salinity-induced potassium efflux in barley root epidermis. Planta. 1 févr 2007;225(3):753‑61.

7. Cuin TA, Betts SA, Chalmandrier R, Shabala S. A root's ability to retain K+ correlates with salt tolerance in wheat. Journal of Experimental Botany. 1 juill 2008;59(10):2697‑706.

8. Shabala S, Pang J, Zhou M, Shabala L, Cuin TA, Nick P, et al. Electrical signalling and cytokinins mediate effects of light and root cutting on ion uptake in intact plants. Plant, Cell & Environment. févr 2009;32(2):194‑207.

9. Shabala S, Shabala S, Cuin TA, Pang J, Percey W, Chen Z, et al. Xylem ionic relations and salinity tolerance in barley. The Plant Journal. mars 2010;61(5):839‑53.

10. Wegner LH, Stefano G, Shabala L, Rossi M, Mancuso S, Shabala S. Sequential depolarization of root cortical and stelar cells induced by an acute salt shock - implications for Na+ and K+ transport into xylem vessels: Salt shock depolarization of root cells. Plant, Cell & Environment. mai 2011;34(5):859‑69.

11. Bose J, Xie Y, Shen W, Shabala S. Haem oxygenase modifies salinity tolerance in Arabidopsis by controlling K+ retention via regulation of the plasma membrane H+-ATPase and by altering SOS1 transcript levels in roots. Journal of Experimental Botany. janv 2013;64(2):471‑81.

12. Teakle NL, Bazihizina N, Shabala S, Colmer TD, Barrett-Lennard EG, Rodrigo-Moreno A, et al. Differential tolerance to combined salinity and O2 deficiency in the halophytic grasses Puccinellia ciliata and Thinopyrum ponticum: The importance of K+ retention in roots. Environmental and Experimental Botany. mars 2013;87:69‑78.

13. Bose J, Shabala L, Pottosin I, Zeng F, Velarde-Buendía A-M, Massart A, et al. Kinetics of xylem loading, membrane potential maintenance, and sensitivity of K + -permeable channels to reactive oxygen species: physiological traits that differentiate salinity tolerance between pea and barley: Mechanisms of salinity tolerance in pea and barley. Plant Cell Environ. mars 2014;37(3):589‑600.

14. Percey WJ, Shabala L, Breadmore MC, Guijt RM, Bose J, Shabala S. Ion transport in broad bean leaf mesophyll under saline conditions. Planta. oct 2014;240(4):729‑43.

15. Bose J, Rodrigo-Moreno A, Lai D, Xie Y, Shen W, Shabala S. Rapid regulation of the plasma membrane H+-ATPase activity is essential to salinity tolerance in two halophyte species, Atriplex lentiformis and Chenopodium quinoa. Annals of Botany. févr 2015;115(3):481‑94.

16. Shabala L, Zhang J, Pottosin I, Bose J, Zhu M, Fuglsang AT, et al. Cell-Type-Specific H + -ATPase Activity in Root Tissues Enables K + Retention and Mediates Acclimation of Barley (Hordeum vulgare) to Salinity Stress. Plant Physiol. déc 2016;172(4):2445‑58.

17. Gill MB, Zeng F, Shabala L, Zhang G, Fan Y, Shabala S, et al. Cell-Based Phenotyping Reveals QTL for Membrane Potential Maintenance Associated with Hypoxia and Salinity Stress Tolerance in Barley. Front Plant Sci. 16 nov 2017;8:1941.

18. Zeng F, Shabala S, Maksimović JD, Maksimović V, Bonales-Alatorre E, Shabala L, et al. Revealing mechanisms of salinity tissue tolerance in succulent halophytes: A case study for Carpobrotus rossi: Salinity tissue tolerance in succulent halophytes. Plant Cell Environ. nov 2018;41(11):2654‑67.

19. Su N, Wu Q, Chen J, Shabala L, Mithöfer A, Wang H, et al. GABA operates upstream of H+-ATPase and improves salinity tolerance in Arabidopsis by enabling cytosolic K+ retention and Na+ exclusion. Sunkar R, éditeur. Journal of Experimental Botany. 18 nov 2019;70(21):6349‑61.

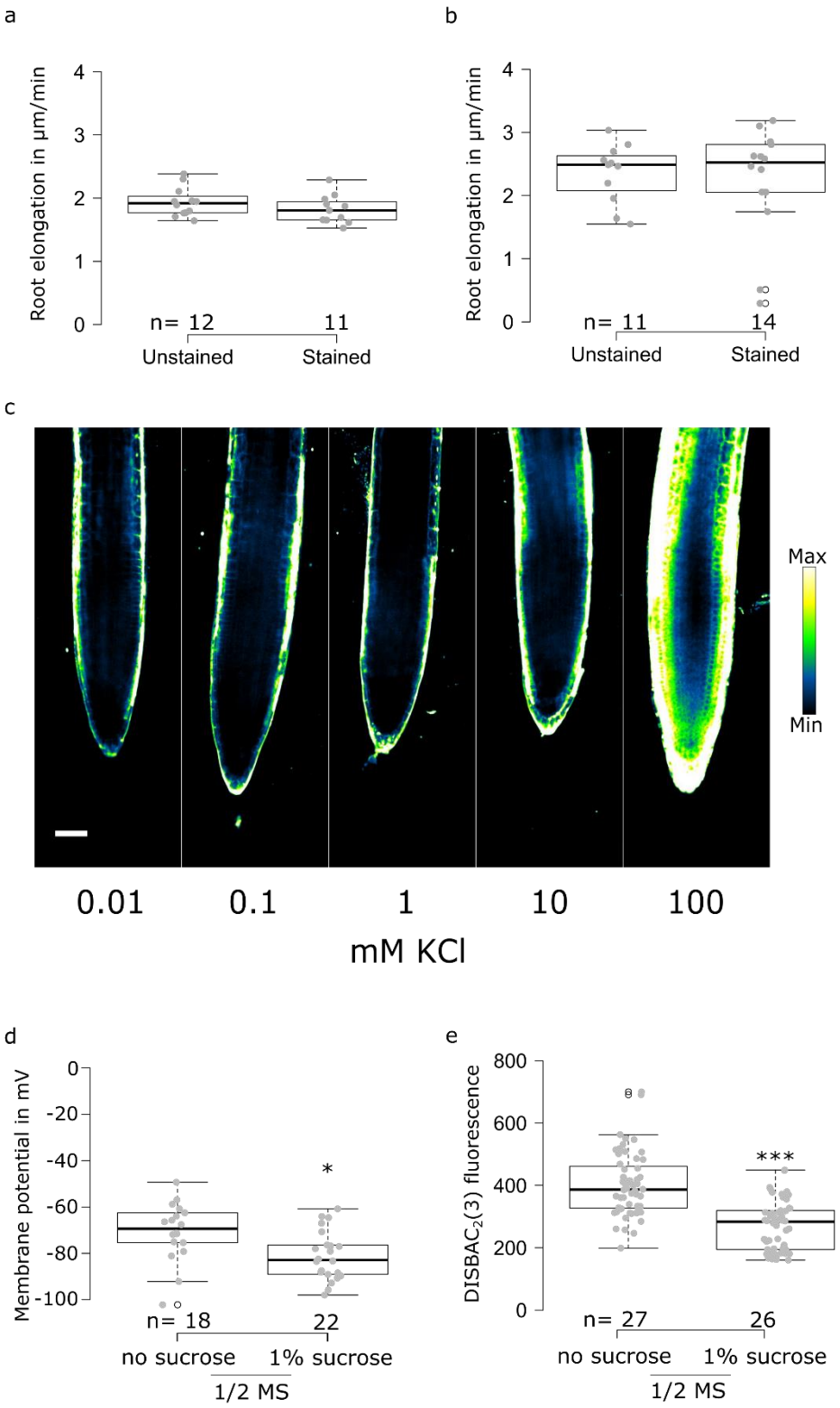

Figure S1. a,b) Effect of DISBAC$_2$(3) staining (0µM and 15µM) on primary root elongation (µm/minute) measured b) every 30 minutes over 10 hours grown on agar surface and b) measured every 5 minutes over 40 minutes and imaged using the spinning disk microscope. c) DISBAC$_2$(3) fluorescence in response to a KCl gradient (0.01 to 100mM by x10 increments). d,e) Effect of sucrose in ½ MS on Col0 membrane potential measured by d) microelectrode and e) DISBAC$_2$(3). Scale bars = 50µm. n= are indicated on figures. (c) Representative microscopy pictures of two independent experiments (median measured values). ***: p-value<0.0005. *: p-value<0.05. Statistical analysis for (a,b,d,e) were conducted with a two-sided non-parametric Student test. ***: p-value<0.0005, **: p-value<0.005, *: p-value<0.05.

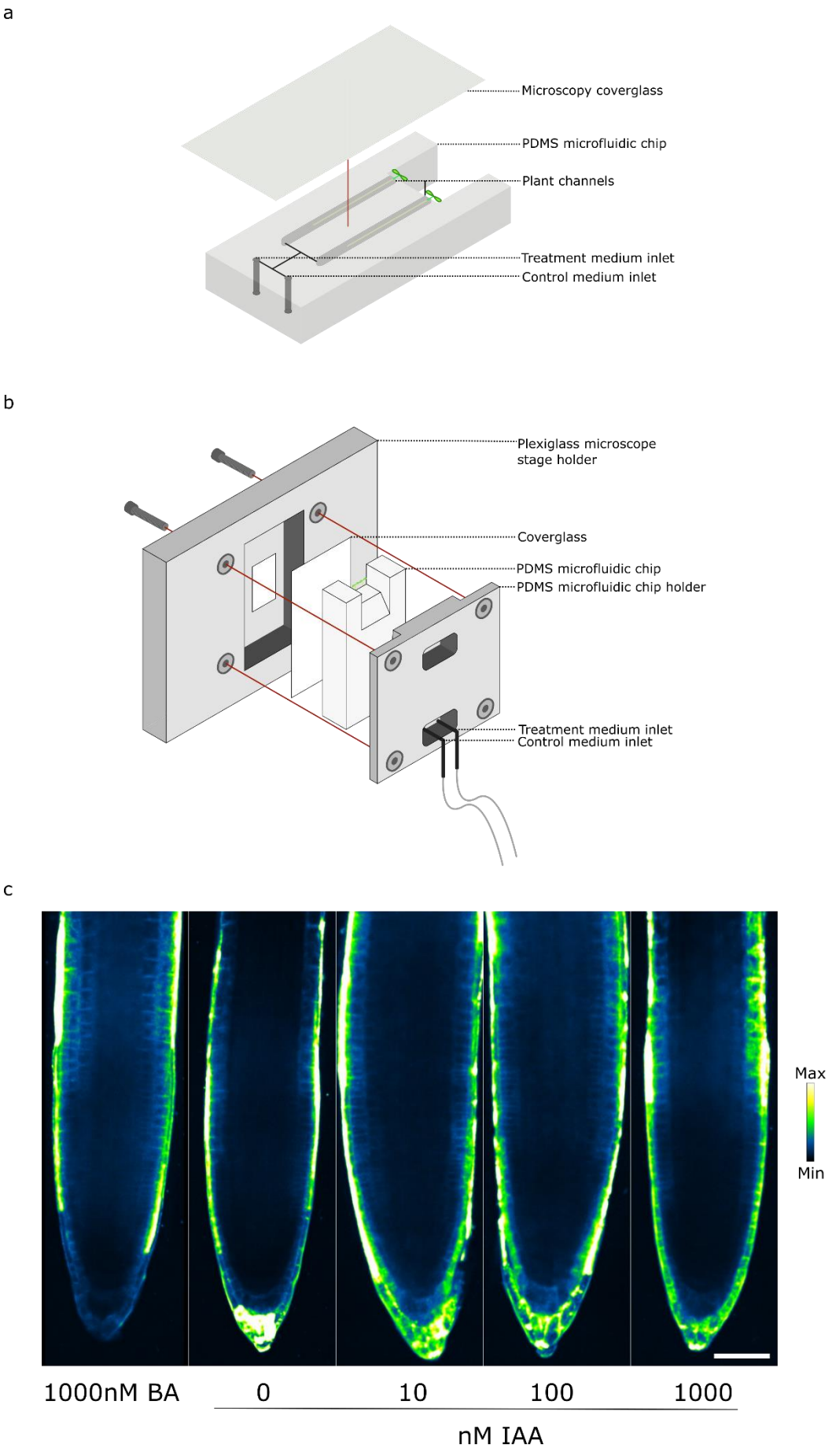

Figure S2. a,b) Schematic of the closable PDMS microfluidic chip. c) Effect of an IAA gradient on Col0 membrane potential after 20 minutes of treatments. Representative microscopy images from two independent experiments (median measured values), fluorescence lookup table indicated next to images. Scale bar = 50µm.

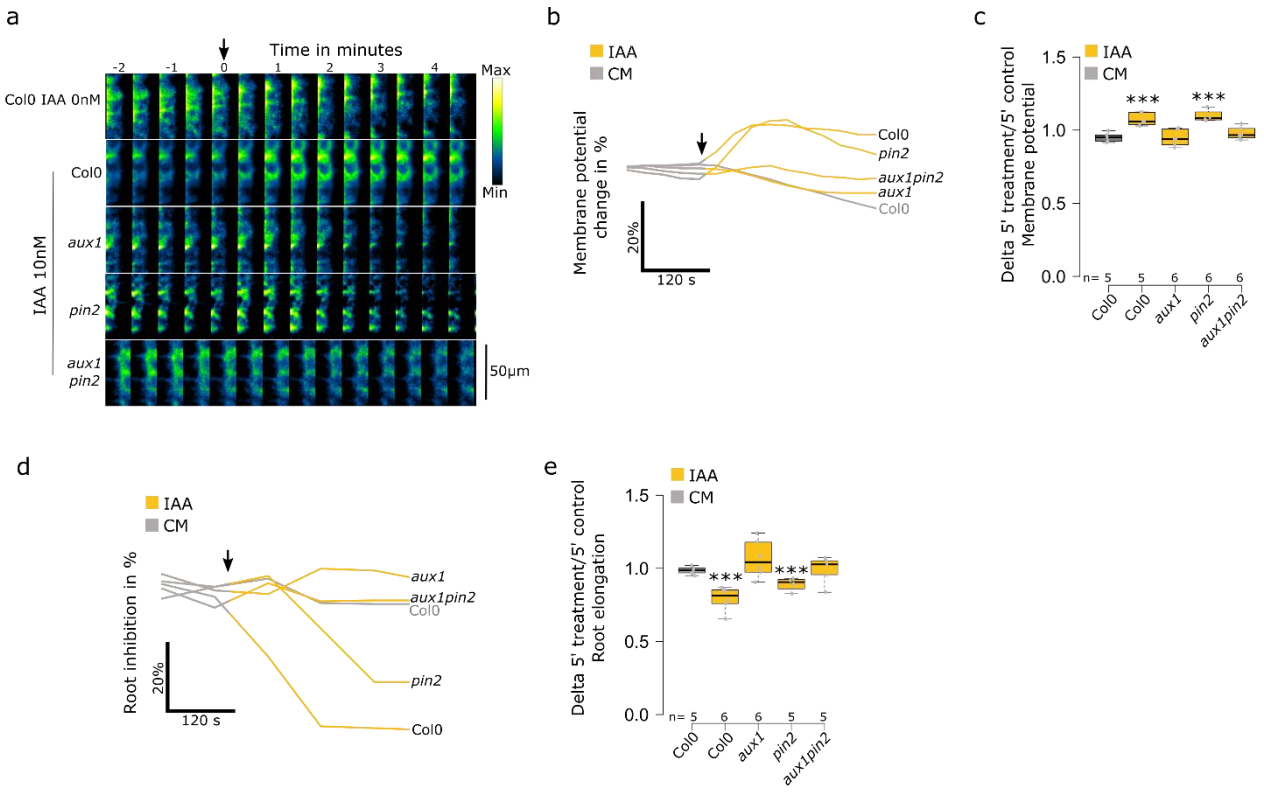

Figure S3. a-e) Effect of 10nM IAA on the rapid response of Col0, *aux1*, *pin2* and *aux1pin2.* a) Representative images of the membrane potential reporter in time. b) Mean change in membrane potential (in %) over 5 minutes of treatment and c) delta of 5 minutes treatment over 5 minutes control media. d) Root elongation over 10 minutes of treatment, mean change (in %) over 5 minutes of treatment and e) delta of 5 minutes treatment over 5 minutes control media. Application of treatments is indicated by a black arrow. For b and d, standard errors were not added to simplify reading. The selected microscopy pictures are representing the median fluorescence value. Fluorescence look up table indicated next to images, scale bar = 50µm. n= is indicated on figures. ***: p-value<0.0005. Statistical analysis for (c,e) were conducted with a two-sided non-parametric multiple comparison with Dunnett contrast and logit approximation. ***: p-value<0.0005, **: p-value<0.005, *: p-value<0.05.

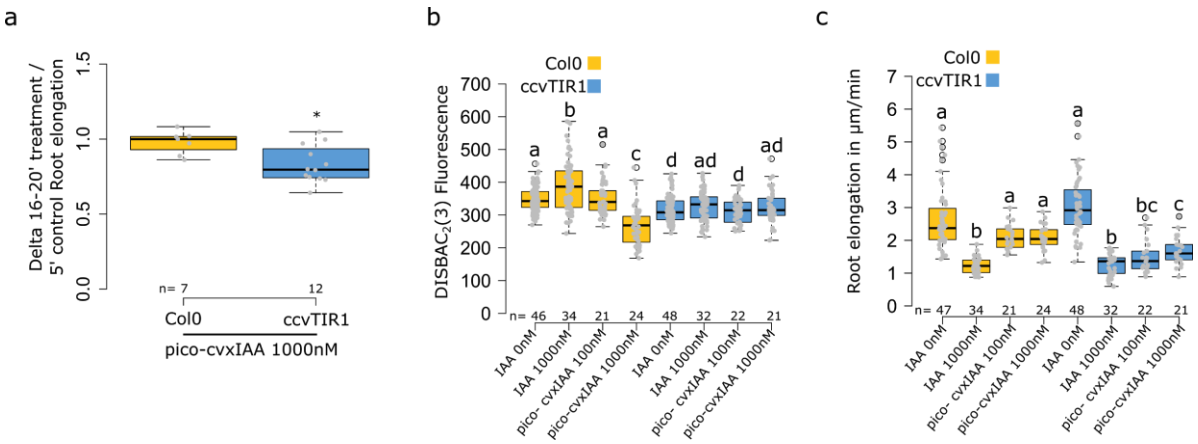

Figure S4. a) Effect of pico-cvxIAA on root elongation ratio of 16-20 minutes treatment over 5 minutes control media during microfluidics experiment. b,c) Effect of IAA and pico-cvxIAA on the steady state response of Col0 and ccvTIR1 b) root tip membrane potential and c) primary root elongation (µm/minute). Steady state corresponds to the fluorescence of roots after 20 minutes of treatment in agar medium and root elongation measured over 40 minutes. n= is indicated on figures. ***: p-value<0.0005, *: p-value<0.05. Statistical analysis for (a) were conducted with a two-sided non-parametric Student test. ***: p-value<0.0005, **: p-value<0.005, *: p-value<0.05. For (b,c) statistics were conducted with a two-sided non-parametric multiple comparison with Tukey contrast and logit approximation. Letters indicates the significantly different statistical group with a p-value<0.05 minimum.

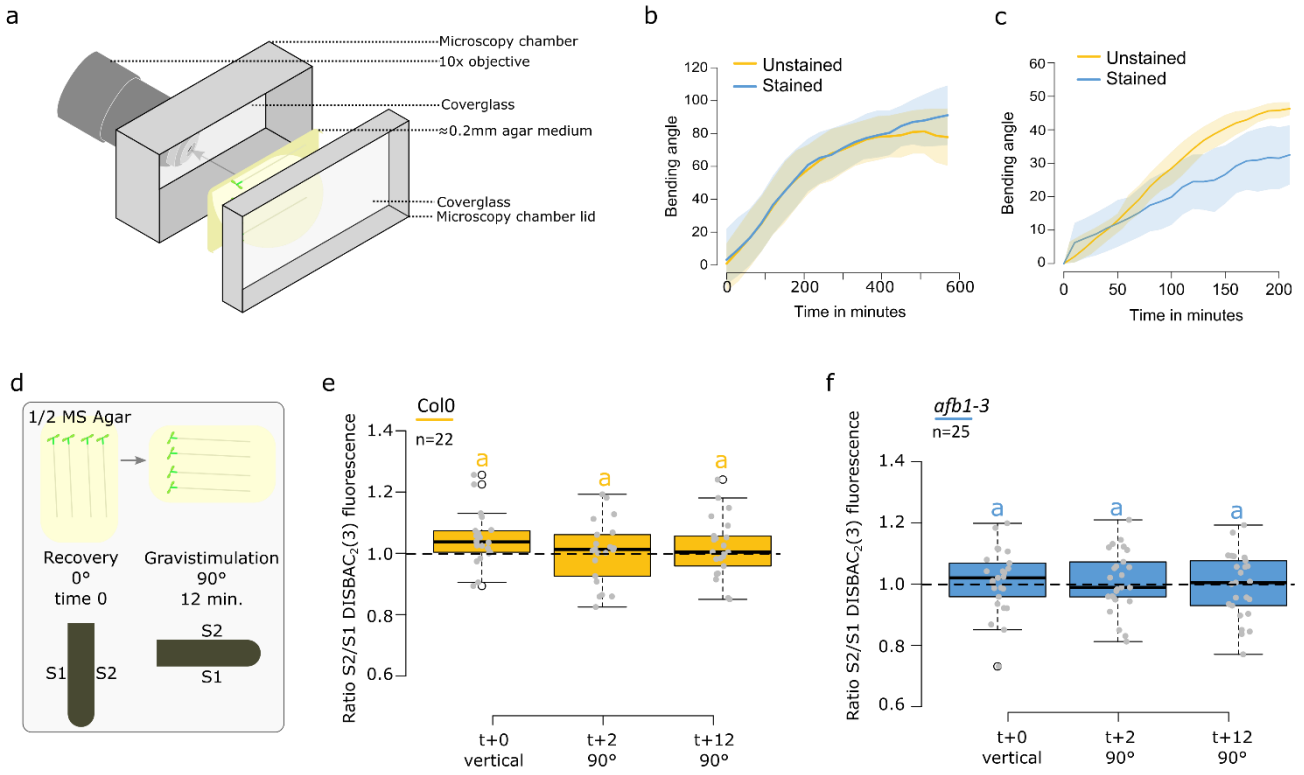

Supplemental 5. a) Schematic of the setup for high spatio-temporal resolution measurements of gravitropic bending with a vertical stage microscope. b),c) Effect of DISBAC$_2$(3) staining (0µM and 15µM) on means +/- SD bending (SD represented as shaded areas) gravitropic root bending b) root tip angle measured every 30 minutes over 10 hours with a flatbed scanner setup and c) measured every 5 minutes over 40 minutes grown in the imaging chamber on the spinning disk microscope. d) Schematic representing the gravitropic experiment: After 25 minutes of recovery, chamber was turned 90° clockwise and imaged for 12 minutes. e),f) Quantification of e) Col0 and f) *afb1-3* transition zone membrane potential ratio S2/S1 after 90° clockwise rotation and S2/S1 after 180° anticlockwise rotation. For (e,f) statistics were conducted with a two-sided non-parametric multiple comparison with Tukey contrast and logit approximation. Letters indicates the significantly different statistical group with a p-value<0.05 minimum.

Supplementary method

Root bending angles for high spatiotemporal gravibending experiments were semi-automatically measured with an ImageJ macro and an R script.

Estimation of the root surface was obtain using an ImageJ macro with manual and automated processes for critical steps. First, the stack of images was stabilized on the root tip (a). Then, the stack was corrected by various image treatments (Bleach correction, Enhance contrast and Creating background,b-e) for more accurate thresholding. The stack was then transformed into a binary image (f) and manually cropped (g). Finally, the root surface (x,y) coordinates of each time frames were exported as a text file (h). Once the root surface coordinates were imported into R by a R script (i), every time frame was individually automatically manipulated to calculate the root bending angle. First, the root perimeter was detected by searching for the maximum (upper side of the root) and minimum (lower side of the root) y values for each individual x values. Root perimeter was represented by one upper and one lower side curve (j). Then, to ensure that all roots and time frames were treated in the same space we normalized the coordinates in space by applying a translation of $y_{minimum}$ and $y_{maximum}$ to x_0 (k). From these two perimeter curves, we estimated the middle of the root by using a polynomial regression of the third degree and its prediction over the $[x_{minimum}:x_{maximum}]$ range (l). Using the upper and lower curves and their intersection points at the root tip, we drew a horizontal line cutting the root tip in two equal parts. The line was passing by the first coordinates of the middle fitting curve (at the root tip) and a point 600 pixels further (shootward) (magenta line, m). The same principle was applied on the mature zone side by drawing a line passing by the maximum middle model value MZ side and a value 600 pixels before (n). This last line was then rotated by 90° and translated in space to be in the middle of the root (o). These last steps ensured that the script could measure both arbitrary negative (upward bending) and positive (downward bending) values. The reference line was only calculated on the first time frame and was used as a reference for each individual root. This translation does not affect is not relevant for root angle per se but is important to have the line into the output graphic. Finally, using the package LearnGeom, the angle (indicated in red on p) between the root tip line (blue line) and the perpendicular line (orange line) was measured. This process was carried out on each root, individually. Once all the angles for one root were calculated, the first angle was subtracted from all the subsequent angles to obtain the relative root bending.

The scripts used for this measurement are available at https://sourceforge.net/projects/gravifast.

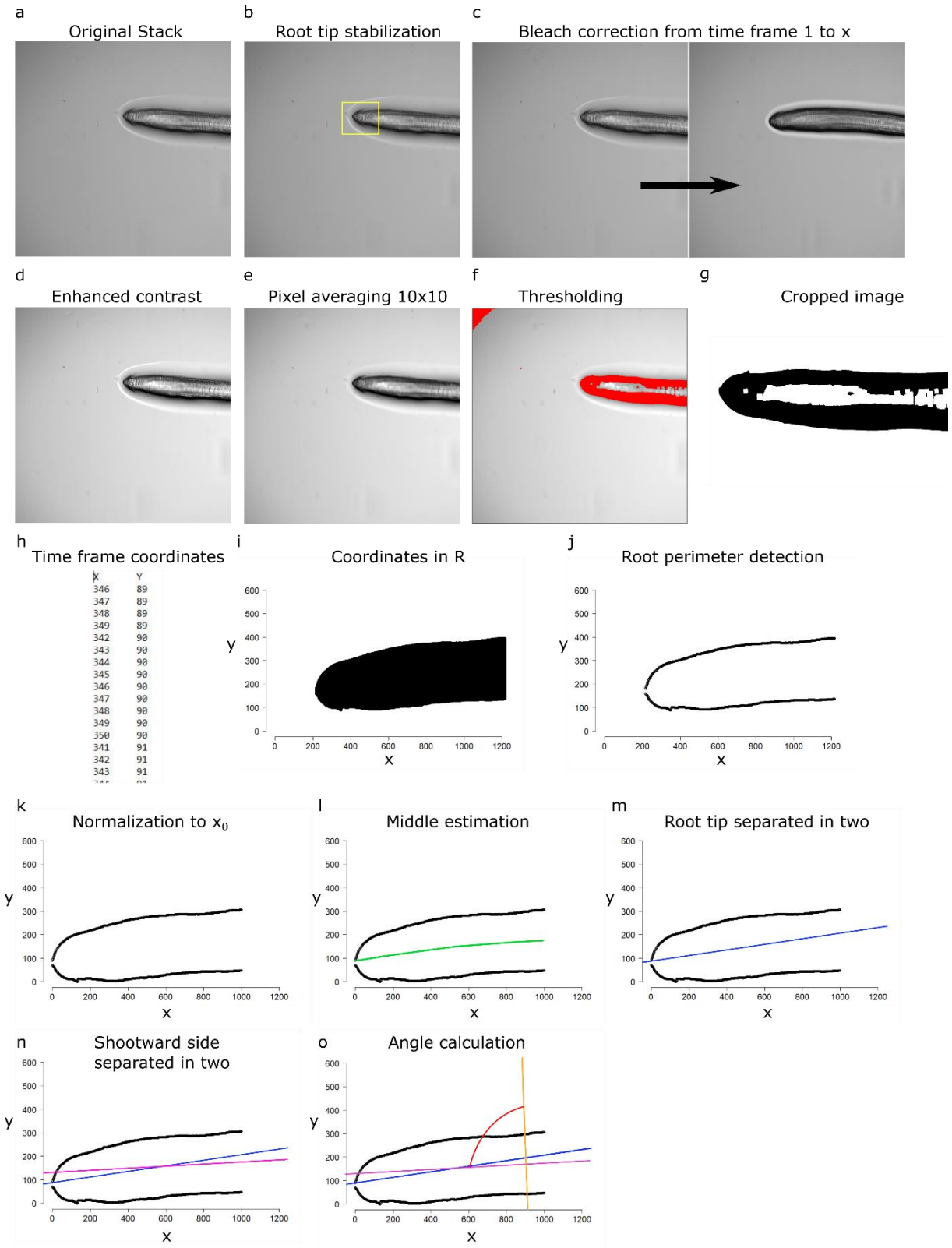

a) Imported original tiff stack
b) Manual rectangular selection of the root tip to automatically apply root tip stabilization
c) Bleach correction to make the background between time frames homogeneous
d) Enhance contrast
e) Pixel averaging 10x10 into one
f) Thresholding
g) Binary and manually cropped image
j) Export of coordinates covering the area of the root in each time frame individually
i) Raw coordinates from ImageJ export plotted in R
j) Isolation of the root perimeter coordinates
k) Normalization by translation to x_0
l) Green line represents the middle of the root obtained by fitting lower and upper side curves with a polynomial of the third degree
m) Blue line is cutting root tip in two equal surfaces
n) Magenta line is cutting the shootward side of the root in two equal surfaces
o) Orange line is a perpendicular line to the green one. The red angle is the calculated angle